



72nd Conference of the Italian Thermal Machines Engineering Association, ATI2017, 6-8 September 2017, Lecce, Italy

Combustion and performance characteristics of air-fuel mixtures ignited by means of photo-thermal ignition of Nano-Energetic Materials

A. Paolo Carlucci, A. Ficarella, D. Laforgia, L. Strafella*

Department of Engineering for Innovation, University of Salento, Lecce 73100, Italy

Abstract

This work presents an experimental investigation to determine the performance and characteristics of the combustion process triggered by a new ignition system based on photo-thermal effect, observed when nano-Energetic Materials are exposed to a flash light. The resulting combustion process has been compared with the one obtained using the spark-plug traditionally used in spark ignition engines.

Results showed that the photo-thermal ignition determines higher combustion pressure gradient, peak pressure, total heat released, fuel combustion efficiency, and a shorter ignition delay and combustion duration compared with the spark ignition, for all the tested fuels and air-fuel ratios.

© 2017 The Authors. Published by Elsevier Ltd.

Peer-review under responsibility of the scientific committee of the 72nd Conference of the Italian Thermal Machines Engineering Association

Keywords: Carbon nanotubes; Ignition; Internal combustion engine; MWCNTs; Photo-thermal ignition; SWCNTs.

1. Introduction

Carbon NanoTubes (CNT) can be ignited with an ordinary camera flash and exhibit photo-thermal heating and ignition properties with relatively low input energy. This phenomenon is usually referred to as “*photo-thermal ignition*” (PTI). The mechanism by which CNTs photo-ignite is difficult to analyze and has not been fully explained.

* Corresponding author. Tel.: +39 0832 297320; fax: +39 0832 297777.

E-mail address: luciano.strafella@unisalento.it

However, there are some theories that try to explain how CNTs undergo the spontaneous ignition when exposed to a light flash, based on several experimental investigations.

The first observation of this phenomenon was documented by Ajayan et al. [1]. They suggested that the optically black SWCNTs fibers absorbed visible and infrared light and transmitted that energy as heat to Fe (iron) nanoparticle sites, which subsequently gained enough activation energy to oxidize and support a combustion reaction with the surrounding air. Tseng et al. in [2] proposed that the photo-acoustic and ignition effects are attributable to rapid increase in temperature over 457°C (ignition point of ferrocene), resulting from absorption of the light flash by CNTs and the presence of catalyst particles in fluffy SWCNTs, generating an acoustic wave and oxidation of the CNTs. Bockrath et al. [3] showed that the phenomenon is not isolated to SWCNTs but in fact, other carbonaceous compounds synthesized on metal catalysts can ignite upon exposure to a flash lamp. Braidy et al. in [4] confirmed the flash ignition effect on SWCNTs but also reported the presence of iron oxide particles in the combustion byproducts. In [5] the Authors concluded that the metal nanoparticle impurities in the SWCNT samples are responsible for the photo-ignition phenomenon.

However, since the first observation of such a phenomenon, few applications of the photo-ignition phenomenon to combustion processes have been proposed. Among them, the idea of igniting various fuel/oxidizer mixtures via traditional thermal ignition induced by the hot photo-ignited nanomaterials has been investigated.

This was demonstrated by Berkowitz et al. in [6]: SWCNTs (containing the 70% iron by weight) introduced and mixed in an air-ethylene mixture inside a combustion chamber and exposed to the camera flash, triggered the combustion process. Another application was proposed by Manaa et al. [7], who demonstrated that the flash ignition and initiation of explosive-nanotubes mixture, like SWCNTs, in solid fuels is possible. However, in order to attain SWCNTs photo-ignition in liquid fuels, the CNTs must be separated from the liquid up ignition occurs. Badakshian et al. [8] have encapsulated a small sample of SWCNTs inside a gelatin capsule through which they have been flashed. It was observed that the photo-ignition of SWCNTs speeded-up the combustion process of hexane + acetone as fuels (50% each). Furthermore, the Authors have also tested photo-ignition of simulated solid rocket fuel (SRF) through photo-ignition of CNTs. In solid rocket motors, in fact, the ignition process generally used is based on the electric ignition. Typically, the hot wire ignites an explosive bag, which rapidly produces hot gases to raise pressure and temperature for the ignition of the solid rocket fuel. This test essentially showed a great potential for the success of the distributed ignition of liquid and solid fuels.

A further application was first suggested by Chehroudi [9] who studied the photo-ignition of liquid fuels with CNTs. Chehroudi believes that this phenomenon could be used to ignite multiple points of an air-fuel mixture simultaneously, for example in internal combustion engines, so realizing the so-called volumetric ignition at the base of Homogeneous Charge Compression Ignition (HCCI) combustion. In previous studies [10-11], the Authors of the present work have compared the combustion process initiated by the nano-ignition agents, when exposed to a light source, with the one obtained with a conventional spark plug ignition system, limiting the analysis to the air-methane mixtures only. For all air-fuel ratios tested, it was demonstrated that the combustion triggered by photo-thermal ignition of the MWCNTs with ferrocene (nano-Energetic materials, nEMs) was characterized by a higher combustion pressure gradient and a higher peak pressure than the one started by a spark-based ignition system. Moreover, a more spatially-homogenous combustion process was observed instead of the classic flame front propagation seen in conventional spark ignition (SI) gasoline engines. Therefore, the investigation has been extended on different fuels, such as LPG, hydrogen and gasoline, without encapsulated MWCNTs/nEMs powder. In this work, the related results are presented and commented.

Nomenclature

MWCNTs	Multi Walled Carbone Nanotubes
SWCNTs	Single Walled Carbone Nanotubes
λ	Air-Fuel Equivalence Ratio
n-EMs	nano-Energetic Materials
PTI	Photo-Thermal Ignition
SI	Spark Ignition

2. Experimental method

As previously said, this study aims to compare the combustion processes of different air-fuel mixtures triggered by two different ignition systems, i.e. PTI and SI.

The ignition agents consisted of MWCNTs powder manually mixed with ferrocene. The amount of ferrocene used is 75% by weight of the total sample weight used in each test. The total weight was equal to 20 mg, since, in preliminary analysis, this was recognized as the minimum amount necessary to trigger the combustion process [11].

To verify whether this new ignition system works with a wide range of fuels, both gaseous and liquid - hydrogen, LPG and gasoline - were used. Results were also compared with those obtained using air-methane mixture during a previous experimental campaign. However, in order to allow operation with both gaseous and liquid fuels, some changes to the early experimental layout described in [10] were necessary.

A schematic diagram of the experimental layout is shown in Fig. 1 (a) for air-gaseous fuels tests and (b) for air-gasoline tests. For air-gaseous fuels tests, the experiments were carried out as described in our previous work [10]. While, for air-gasoline tests, the experiments have been carried out as described in the following. The gasoline injection system is composed of a fuel tank pressurized with an inert gas (nitrogen) to a value equal to 4.5 barg for all tests. The fuel injection system is composed of a traditional automotive gasoline injector and a high-speed Digital Output National Instruments® module to control the injector opening. In order to run the experiments, air and liquid fuel were separately introduced into the combustion chamber. The amount of liquid fuel introduced into the combustion chamber was determined to ensure a desired value of the air-gasoline ratio. Therefore, the gasoline injector has been thoroughly characterized so that the amount of gasoline per injection was known for each test. The amount of liquid fuel introduced was changed varying the pulse width applied to the injector control system. Once the gasoline was injected into the combustion chamber, the air - filling the mixture chamber at a pressure of 6 barg - has been introduced into the combustion chamber by means of a solenoid valve. The amount of air introduced into the combustion chamber was controlled by the opening time of the solenoid in order to reach the desired pressure of 3 barg for each test. In this case, the MWCNTs/nEMs, previously placed in the CNTs holder, have been introduced into the combustion chamber only by the air flow.

At the end of each test, the combustion chamber was thoroughly purged with fresh air before starting a new one.

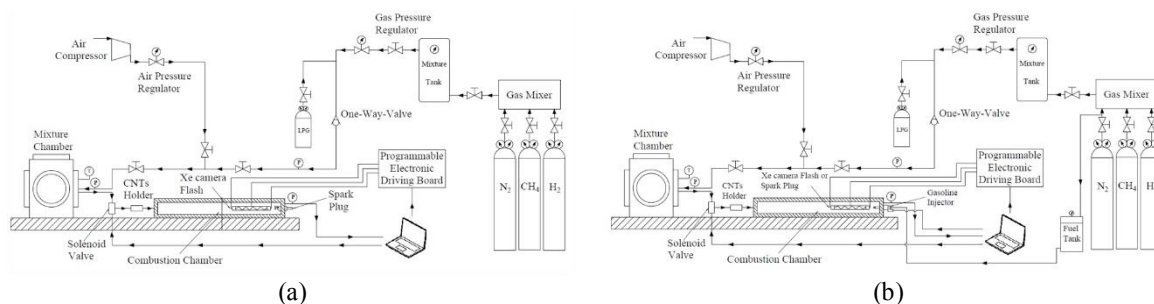


Fig. 1. Scheme of the experimental apparatus used during (a) air-gaseous fuels and (b) air-gasoline fuel tests.

The constant-volume mixture chamber is made of low-carbon steel and has a cylindrical shape with inner diameter of 53 mm and length of 270 mm. The chamber is equipped with a piezoresistive pressure sensor (KELLER type PA-21Y 0-200 bar). Pressure signal has been sampled at 2.5 kHz using a NI cDAQ 9178 acquisition board with a NI 9205 AI module, and processed through LabVIEW NI software. A longitudinal quartz rectangular optical window (172 mm length x 37 mm height x 20 mm thickness) allows visual access inside the combustion chamber and is mounted along the combustion chamber. A CCD Memrecam GX-1F High Speed framing camera is positioned in front of the quartz optical access and the images of the ignition and burning processes have been acquired with a frame rate equal to 2.5 kHz.

An automotive spark plug (NGK model 4983 DCPR7E-N-10), a Xe camera flash (SIGMA model EF-610DGST for air-gaseous fuel tests, and a Linear Xenon Flash Tubes model FT-L6085 for air-gasoline tests) are placed at appropriate locations inside the combustion chamber (see Fig. 1). In this manner, the combustion process via spark

plug ignition of the mixture can be compared with that obtained through ignition of MWCNTs/nEMs mixed with air-fuel mixture. Both PTI and SI ignition methods have been activated by a relay, remotely controlled by means of a DIO 5 Volt TTL High Speed NI 9401 module. Once the desired combustion chamber pressure (3 barg) is reached, the solenoid valve automatically closes and, after a constant delay time, a TTL signal is generated for activating either the camera flash or the spark plug. The energy released by the flash unit was about 5 J for air-methane fuel tests (this value has been assumed constant and taken as reference for all air-gaseous fuel tests) and 8 J for air-gasoline tests. The energy released by the spark plug was about 20 J for all tests.

Results by the PTI have been compared with those obtained igniting the same air-gaseous fuel mixture with a conventional spark plug. Similar results for the air-gasoline mixtures will be discussed.

3. Results and discussion

3.1. Combustion Analysis

For both PTI and SI ignition systems, tests were conducted by varying the air-fuel equivalence ratio, λ , defined as:

$$\lambda = \frac{(A/F)_{act}}{(A/F)_{st}} \quad (1)$$

where $(A/F)_{act}$ is the ratio between air and fuel mass actually filling to the combustion chamber, while $(A/F)_{st}$ is the stoichiometric ratio between air and the type of the fuel used. In this work, $(A/F)_{st}$ for methane, hydrogen, LPG, and gasoline were set equal to 17.24, 34, 15.5, and 14.7, respectively. The air-fuel equivalence ratio, λ , was varied within a range from 1 to 4. The ignition and combustion characteristics were analyzed through measurement of the combustion chamber pressure. In fact, for a constant volume chamber and under the hypotheses of homogeneous system and negligible wall heat transfer, the 1st Law of Thermodynamics allows to estimate the rate of heat released (*HRR*) by the fuel through the following expression [11]:

$$HRR = \frac{dQ}{dt} = \frac{1}{\gamma - 1} V \frac{dp}{dt} \quad (2)$$

where Q is the heat released by the fuel during combustion (on first approximation proportional to the fuel burned), γ is the mixture specific heat ratio (fixed constant and equal to 1.38), V is the combustion chamber volume and p is the measured pressure.

Thanks to the calculation of the heat release rate, it is also possible to estimate the thermal energy released or the total heat released during combustion calculating the cumulative time histories of the *HRR* as follows:

$$cumHRR = \int_{t_{ignition}}^{t_{pmax}} HRR dt \quad (3)$$

The thermal energy released is the final value of *cumHRR* implemented only during the rising phase of the time history of the chamber pressure ($t_{pmax} - t_{ignition}$). In fact, only the rising phase is representative of the combustion process development, since the falling portion of curve is due to cooling of the exhaust gases due to heat exchanged with the chamber walls. Furthermore, thanks to the calculation of the heat release rate, it is also possible to estimate the combustion efficiency, defined as:

$$\eta_b = \frac{cumHRR}{m_{fuel} H_{i,fuel}} \quad (4)$$

in which the numerator is equal to the thermal energy released or total heat released during combustion, while the denominator is equal to the thermal energy supplied to the system in the form of liquid or gaseous fuels.

An example of data acquired during experiments is reported in Fig. 2, where combustion *cumHRR* traces obtained through ignition of MWCNTs/nEMs or a spark plug in an air-methane mixture with a λ value of 1.58 are shown. It is possible to see that, after the trigger signal (flash or spark activation), both curves exhibit a rising phase, due to the heat released by the fuel during the combustion, and reach a peak value when all the fuel has burned.

From the heat released curves, it was possible to estimate:

- the *ignition delay*, defined as the difference between the time when the heat released had reached a value equal to 10% of the total heat released and the time when the trigger has been activated;
- the *combustion duration*, defined as the difference between the times when the heat released had reached 90% and 10% of the heat released. The “total” combustion period is, on the other hand, the sum of “*ignition delay*” and “*combustion duration*”.

From Fig. 2, it can be observed that the combustion initiated by the MWCNTs/nEMs photo-thermal ignition evolves more rapidly, exhibits a shorter ignition delay period, and leads to a total heat released higher than the case in which the mixture is ignited by a spark plug. This last effect is thought to be due to two reasons. On one hand, the wall heat transfer is expected to play a role in SI due to longer combustion duration. On the other hand, analyzing the combustion process images (see results presented in the following section), the combustion triggered by PI involves more quickly the whole mixture in the combustion chamber if compared to SI: in this way, the mixture at the peripheral areas of the combustion chamber are expected to be more easily reached and burned. While for SI triggered combustion, this would happen more hardly because the flame front cools as it approaches the walls of the chamber.

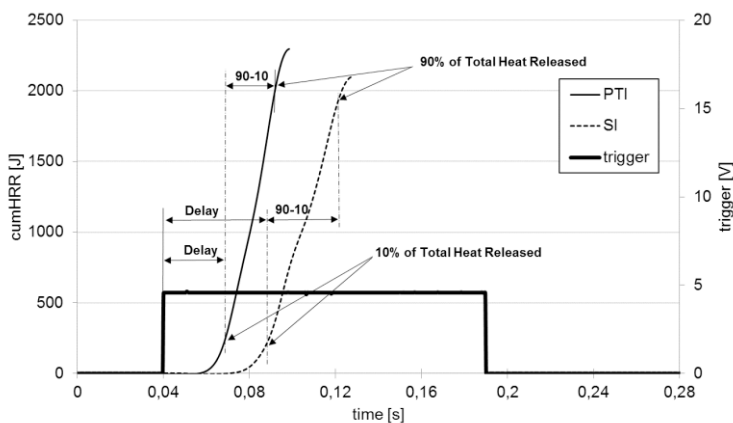


Fig. 2. Cumulative Heat Released traces with MWCNTs/nEMs photo-thermal ignition and with spark ignition of an air-methane mixture at $\lambda = 1.58$.

3.2. Investigation on air-fuel mixtures

As previously described, several air-fuel mixtures have been tested with the aim to demonstrate the feasibility to ignite them by means of the photo-thermal ignition phenomenon in a constant-volume combustion chamber; the combustion process has been compared with the one obtained with a traditional spark ignition system.

In Fig. 3 the results characterizing the combustion processes related to MWCNTs/nEMs-ignition and spark-ignition in terms of combustion duration and ignition delay (a-a'-a''-a'''), total heat released and pressure peak (b-b'-b''-b''') and efficiency percentage variation (c-c'-c''-c''') for all fuels tested are reported for different values of λ . A visual comparison of the results suggests that the peak combustion chamber pressure reached when the mixture is ignited

with MWCNTs/nEMs is always higher or comparable to that observed using the spark plug. Increasing the value of λ , i.e. burning leaner mixtures, the peak of total heat released and combustion pressure both decrease. It can also be seen that, with MWCNTs/nEMs, both ignition delay and combustion duration are shorter.

It is possible to note that the heat released and combustion pressure peak value assume the highest value with $\lambda=1$ and both decrease at $\lambda>1$. This is because the amount of air to complete the combustion process is more than that necessary for the stoichiometric air-fuel ratio ($\lambda=1$) and the thermal energy released from fuel is lower. Finally, it is possible to note that the combustion efficiency obtained from the combustion process triggered by photo-thermal ignition is almost always higher to that observed using the spark plug, for each fuel tested.

It can also be observed, for gasoline tests, that the combustion process for leanest tested condition, that is $\lambda=2.76$, has occurred only for the PTI process, while a misfire took place when combustion was initiated by the spark-plug system. This misfire could be due to either an excess of air in the air-fuel mixture or the nature of the spark-plug ignition process. Since the spark plug can only provide ignition at a single point, the flame front is unable to propagate throughout this very lean mixture.

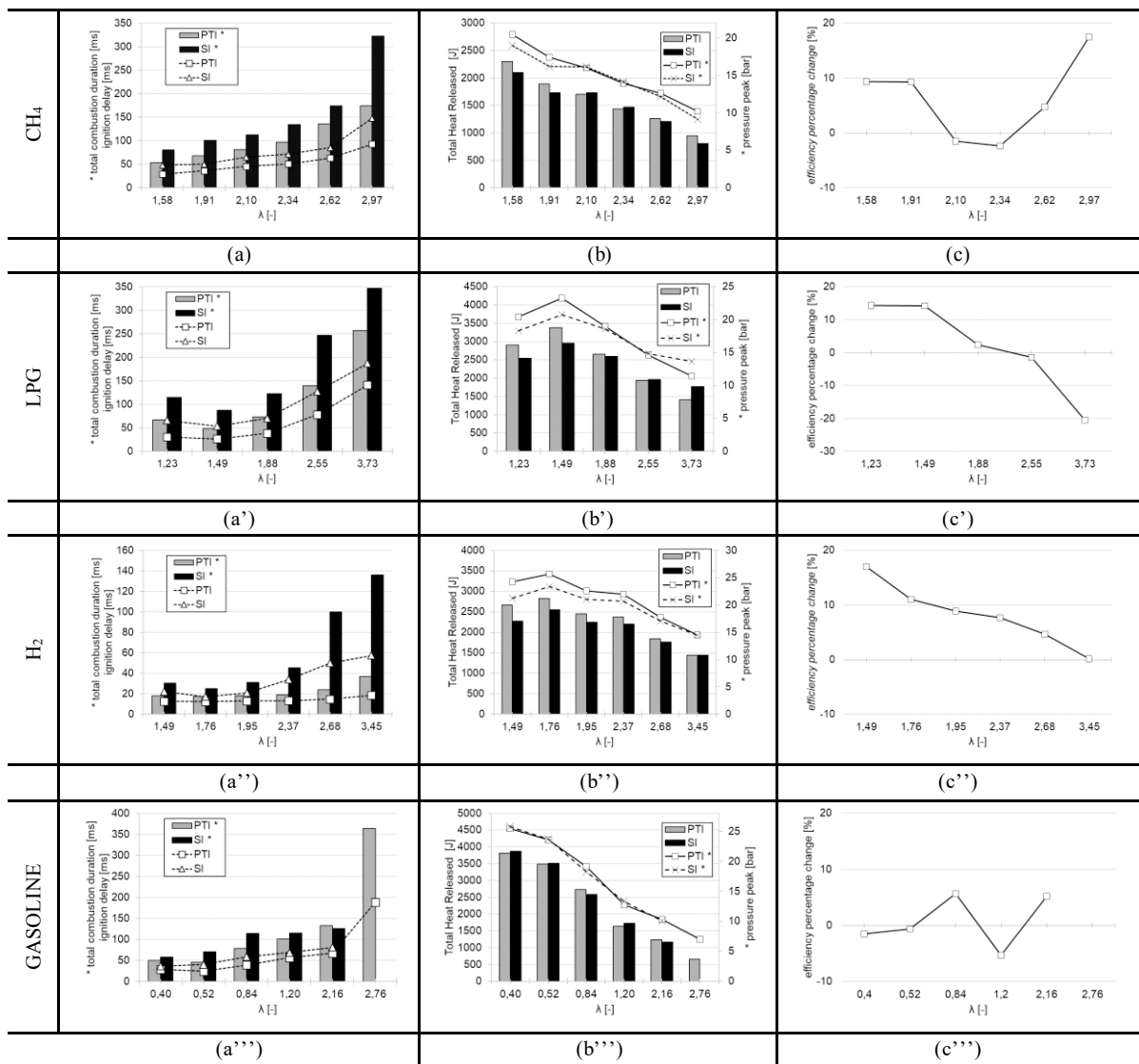


Fig. 3. Combustion duration and ignition delay (a-a'-a''-a'''), total heat released and pressure peak (b-b'-b''-b''') and efficiency percentage change (c-c'-c''-c''') for all fuels tested.

For each tests, a higher *cumHRR* and pressure peaks were determined by the fact that the ignition of the mixture by MWCNTs/nEMs flash exposition leads to more ignition nuclei burning “simultaneously”, so speeding up and powering the combustion process. With the spark plug, as well known, combustion is triggered in only one point, and then proceeds with the propagation of a flame front. The fuel mixture, therefore, is far from burning simultaneously. This behavior has been confirmed by acquiring some images during the combustion process and post-processing them in LabVIEW software with a toolkit to create color maps images. In this way, a false color was assigned to the pixels with the same luminance value, derived from images, by creating a map of colors with the same value. From Fig. 4 is possible to note how the combustion process triggered by the photo-thermal ignition exhibits an instantaneous ignition of the mixture inside the combustion chamber reaching its maximum intensity at about 20 ms after the flash is turned off. Furthermore, the combustion process involves the entire combustion chamber. This could be due to the fact that the ignition nuclei, spatially distributed inside the chamber, are able to ignite the mixture away from the ignition source. On the contrary, the ignition process triggered by spark-plug only involves at the beginning a small fraction of the charge distributed within the chamber with the high intensity areas close to the trigger point (i.e. spark plug), and later the classic propagation of the flame front.

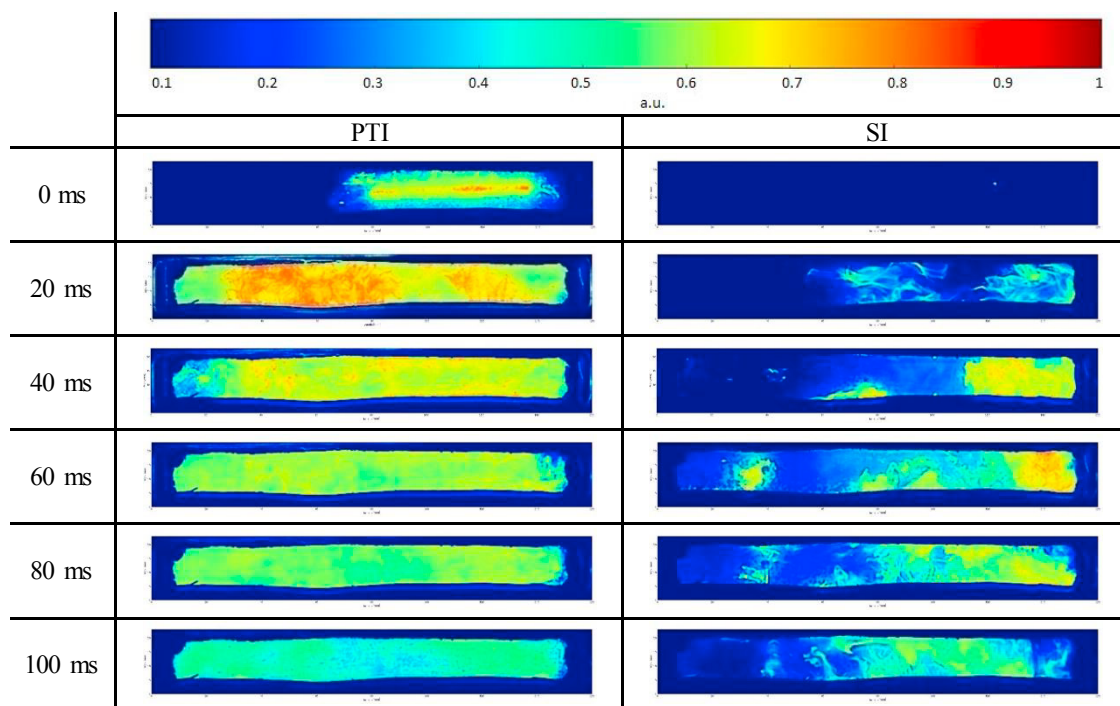


Fig. 4. Color map sequence of the combustion process at $\lambda = 0.52$; comparison between photo-thermal ignition and spark ignition for air-gasoline fuel mixture.

4. Conclusions

An extensive experimental campaign has demonstrated the feasibility of a new ignition concept of the combustion process for several air-fuel mixtures. The new ignition concept, consisting in flashing MWCNTs/nEMs powder with a light source, has been compared with the traditional spark-plug system. The new light-activated distributed ignition demonstrated superior performance in shortening combustion duration and ignition delay and increasing pressure peak and combustion efficiency during the combustion process of air mixed with different fuels - both gaseous and liquid - mixed with different air-fuel ratios. Higher pressure and total heat released peaks are determined by the fact that PTI

leads to more ignition nuclei burning simultaneously, contributing to more volumetrically distributed combustion process into the combustion chamber, differently than the flame front propagation observed with the spark ignition. Finally, it is important to emphasize that the light-activated volumetrically-distributed ignition is able to ignite for the first time, air-gasoline fuel mixtures, without encapsulating MWCNTs/nEMs powder to make them liquidproof, in a constant volume chamber.

The use of the photo-thermal ignition system has the following advantages compared to the other ignition systems:

- the ignition could be achieved remotely and is distributed spatially at a large number of locations;
- the volume within which ignition takes place can be adjusted to achieve both localized and volumetrically-distributed ignition.

Therefore, it is a strongly candidate as alternative ignition source for more efficient and performing future engines.

References

- [1] Ajayan PM, Terrones M, de la Guardia A. (2002) “Nanotubes in a flash-ignition– ignition and reconstruction”. *Science* 296, (2002): 705.
- [2] Tseng S, Tai N, Hsu W, Chen L, Wang J, Chiu C. (2007) “Ignition of carbon nanotubes using a photoflash”. *Carbon* 45.5 (2007): 958-964.
- [3] Bockrath B, Johnson JK, Sholl DS, Howard B, Matragna C, Shi W. (2002) “Ignition Nanotubes with a Flash”. *Science* 297.5579 (2002): 192-193.
- [4] Braidly N, Botton GA, Adronov A. (2002) “Oxidation of Fe nanoparticles embedded in single-walled carbon nanotubes by exposure to a bright flash of white light”. *Nano Letters* 8 (2002): 1277-1280.
- [5] Smits J, Wincheski B, Namkung M, Crooks R, Louie R. (2003) “Response of Fe powder, purified and as-produced HiPco single-walled carbon nanotubes to flash exposure”. *Materials Science and Engineering: A (Structural Materials: Properties, Microstructure and Processing)* 358 (2003): 384-389.
- [6] Berkowitz A, Oehlschlaeger M. (2011) “Photo-induced ignition of quiescent ethylene/air mixtures containing suspended carbon nanotubes”. *Proceedings of the Combustion Institute* 33.2 (2011): 3359-3366.
- [7] Manaa R, Mitchell A, Garza R. (2005) “Flash ignition and initiation of explosives nanotubes mixture”. *Journal of the American Chemical Society* 127 (2005): 13786-13787.
- [8] Badakhshan A, Danczyk SA, Wirth D, Pilon L. (2011) “Ignition of liquid fuel spray and simulated solid rocket fuel by photo-ignition of carbon nanotubes utilizing a camera flash”. *JANNAF Liquid Propulsion Conference*, 2011.
- [9] Chehroudi B. (2012). “Nanotechnology and applied combustion: Use of nanostructured materials for light-activated distributed ignition of fuels with propulsion applications”. *Recent Patents on Space Technology* 1.2 (2012): 107-122.
- [10] Carlucci AP, Strafella L. (2015) “Air-methane mixture ignition with Multi-Walled Carbon NanoTubes (MWCNTs) and comparison with spark ignition” *Energy Procedia* 82 (2015): 915-920.
- [11] Carlucci AP, Ciccarella G, Strafella L. (2016) “Multi-Walled Carbon Nanotubes (MWCNTs) as ignition agents for air/methane mixtures” *IEEE Transactions on Nanotechnology* 15.5 (2016): 699-704.